Acetylcholine receptor channel structure in the resting, open, and desensitized states probed with the substituted-cysteine-accessibility method

Gary G. Wilson and Arthur Karlin*

Center for Molecular Recognition, Columbia University, 630 West 168th Street, New York, NY 10032

This contribution is part of the special series of Inaugural Articles by members of the National Academy of Sciences elected on April 27, 1999.

Contributed by Arthur Karlin, November 30, 2000

The nicotinic acetylcholine (ACh) receptors cycle among classes of nonconducting resting states, conducting open states, and nonconducting desensitized states. We previously probed the structure of the mouse-muscle ACh receptor channel in the resting state obtained in the absence of agonist and in the open states obtained after brief exposure to ACh. We now have probed the structure in the stable desensitized state obtained after many minutes of exposure to ACh. Muscle-type receptor has the subunit composition $\alpha_2\beta\gamma\delta$. Each subunit has four membrane-spanning segments, M1–M4. The channel lumen in the membrane domain is lined largely by M2 and to a lesser extent by M1 from each of the subunits. We determined the rates of reaction of a small, sulfhydryl-specific, charged reagent, 2-aminoethyl methanethiosulfonate with cysteines substituted for residues in αM2 and the αM1–M2 loop in the desensitized state and compared these rates to rates previously obtained in the resting and open states. The reaction rates of the substituted cysteines are different in the three functional states of the receptor, indicating significant structural differences. By comparing the rates of reaction of extracellularly and intracellularly added 2-aminoethyl methanethiosulfonate, we previously located the closed gate in the resting state between αG240 and αT244, in the predicted M1–M2 loop at the intracellular end of M2. Now, we have located the closed gate in the stable desensitized state between αG240 and αL251. The gate in the desensitized state includes the resting state gate and an extension further into M2.

The nicotinic acetylcholine (ACh) receptors cycle among three classes of functional states: resting, open, and desensitized (1). The receptor is conducting in the open state and nonconducting in the resting and desensitized states. The resting state is the most stable state when no agonist is bound, whereas the desensitized state is the most stable state when agonist is bound. Muscle-type ACh receptors have two ACh binding sites corresponding to the two α subunits in the pentameric complex (Fig. 1, refs. 2 and 3). In the prevailing cycle of transitions, receptors in the resting state bind two molecules of ACh, isomerize to the open state, and, in the continued presence of ACh eventually desensitize. After the removal of free ACh and its dissociation from the binding sites, receptors in the desensitized state predominantly isomerize directly to the resting state. This cycle of activation, desensitization, and recovery has been extensively studied electrophysiologically (1, 4–7). The role of desensitization in cholinergic neurotransmission under normal physiological conditions is uncertain but is evident under some pathological conditions and in neurotransmission by other neurotransmitters (8).

Desensitization occurs in stages (9). Receptor isomerizes to a transient, fast-onset desensitized state on the 0.1- to 10-s time scale and to a stable, slow-onset desensitized state on the 10- to 100-s time scale (10–17). The ACh affinities of the transient, fast-onset and stable, slow-onset desensitized states are, respectively, 2 and 4 orders of magnitude greater than the affinity of the resting state (18, 19).

The structural bases for the functional properties of the ACh receptors have been investigated by various means. Two-dimensional crystalline arrays of receptors in Torpedo electrocyte membrane have been analyzed by cryo-electron microscopy, and, although the functionality of the receptors in these arrays was undetermined, aspects of the structures in the long-term presence of ACh (putative desensitized state) (20) and in the short-term presence of ACh (putative open state) (21) were different from the structure in the absence of ACh (putative resting state). In particular, the structures of possible ACh-binding sites in the α subunits were different in the presence and absence of ACh (22), and kinks in five membrane-spanning rods were inferred to block the channel in the absence of ACh and to move out of the way within milliseconds after the addition of ACh (21).

Changes in the chemical reactivities of amino acid side chains have long been used to probe structural changes in proteins. In the ACh receptor from Torpedo electrocytes there were marked differences between the resting and desensitized states in the susceptibility of the ACh-binding site disulfide bond (23) to reduction (24) and in the photolabeling of ACh-binding site residues (25). Desensitization changed the extent of incorporation of hydrophobic photolabels into the membrane-spanning domain of the receptor, altered the distribution of the labeling among the subunits, and changed the pattern of labeling in the channel-lining, membrane-spanning segment, M2 (Fig. 1) (26–29).

Noncompetitive inhibitors bind stoichiometrically within the conduction pathway, and the labeling of the membrane-spanning segments with photoactivated noncompetitive inhibitors was quite different in the resting and the desensitized states (29, 30). Also, differences between the resting and the open states were observed in rapid-mixing photolysis experiments with photoactivated noncompetitive inhibitors (31–33).

Mutations of residues in various parts of the receptor were found to alter the rates of channel opening and closing or desensitization. A number of mutations were found to alter the extent or rate of desensitization of muscle-type and neuronal-type receptors. These were in the extracellular domain (34–36) and in the M2 (37–46), M3 (47, 48), and M4 (49) membrane-spanning segments. The mutated residues could take part in the

Abbreviations: ACh, acetylcholine; MTSEA, 2-aminoethyl methanethiosulfonate; SCAM, substituted-cysteine-accessibility method.

*To whom reprint requests should be addressed. E-mail: ak12@columbia.edu.

Article published online before print: *Proc. Natl. Acad. Sci. USA*, 10.1073/pnas.031567798. Article and publication date are at www.pnas.org/cgi/doi/10.1073/pnas.031567798

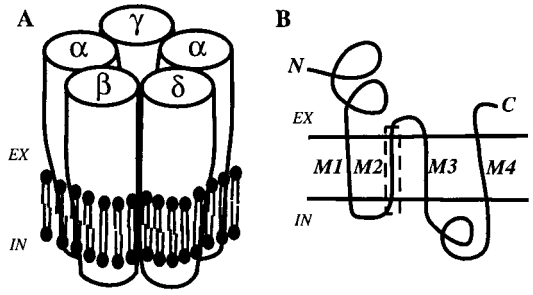

Fig. 1. The arrangement of the ACh receptor subunits (*A*) and their common topology (*B*). The extracellular (EX) and intracellular (IN) sides of the membrane are indicated. The region of Cys substitution is enclosed in a dashed rectangle.

structural transitions between states, although indirect effects of the mutations on expression and folding have not, in most cases, been ruled out. In addition to the above alterations in residues, phosphorylation of residues in the M3–M4 cytoplasmic loop also affects desensitization (50).

The substituted-cysteine-accessibility method (SCAM) is an approach to the characterization of channel structure (51–53) and binding-site structure (54–56) that probes the environment of any residue by mutating it to Cys and by characterizing the reaction of the Cys with sulfhydryl-specific reagents. Both because of the polarity of the methanethiosulfonates used (51, 54) and because these reagents react at least 10 orders of magnitude faster with ionized thiolates than with unionized thiols (57), the reactions are directed to Cys at the water-accessible surface of the protein. Small, charged reagents can serve as surrogates for permeant ions within a channel (51). Their reactions with Cys substituted in membrane-spanning segments can be sensitively monitored electrophysiologically by the effects of the reactions on current. The relative reactivities of substituted Cys can be used to identify channel-lining residues, determine the accessibility of these residues in conducting and nonconducting states of the channel, assess secondary structure, locate selectivity filters and gates, map binding sites within the channel, and estimate the electrostatic potential in the vicinity of accessible residues (53).

In the application of SCAM to the mouse-muscle ACh receptor, each residue in the M1 and M2 membrane-spanning segments and in the M1–M2 loop of both the α subunit and the β subunit was mutated to Cys and probed with charged methanethiosulfonate derivatives. Of 106 Cys-substitution mutants expressed in *Xenopus* oocytes or HEK 293 cells, 105 appeared at the cell surface and conducted cations when activated by ACh, 38 reacted with at least one charged methanethiosulfonate, and 24 reacted with appreciably different rate constants in the resting and open states of the receptor (52, 58–61). The reactivities of the substituted Cys were different in the resting and open states in the N-terminal third of the M1 segments, close to the extracellular side of the membrane, and along the entire length of the M2 segments. Clearly, the molecular environments of the channel-lining residues are different in the resting and open states. By comparing reaction rates of extracellularly and intracellularly added 2-aminoethyl methanethiosulfonate (MTSEA), we were able to locate the resting gate[†] of the channel in the vicinity of αE241, close to the intracellular end of the M2 segment (62). One of the consequences of the closing of this gate is that the large, negative intrinsic electrostatic potential in the open channel, which itself is almost entirely due to αE241 and the aligned glutamates in the other subunits, changes by about 100 mV in the positive direction (61, 63).

Although the channel is closed in both the desensitized states and the resting state, the evidence, reviewed above, indicates that the structures of the channel in these states are different. In addition, the gate in the transient desensitized state was postulated to be different from the gate in the resting state (7). In this paper, we report our use of SCAM to investigate further the structure of the channel in the stable desensitized state and to compare this structure to the structures in the resting and open states. We report the rate constants of the reactions of MTSEA with accessible substituted Cys in αM2. Several rate constants were different in the desensitized state than in either the open state or resting state. One conclusion from the pattern of reactivities is that the gate is more extensive in the desensitized state than in the resting state.

Methods

Molecular Biology and Expression. Cysteine mutants of the M2 segment of mouse muscle α subunit and wild-type α, β, γ and δ subunits were constructed in the pSP64T plasmid for expression in *Xenopus* oocytes and in the pCIneo plasmid for expression in HEK 293 cells as described (62).

Reaction of Extracellularly Applied MTSEA with Desensitized Receptor. The currents evoked by ACh were recorded from voltage-clamped *Xenopus* oocytes as described (63). Oocytes were continuously perfused by a bath solution of 115 mM NaCl, 2.5 mM KCl, 1.8 mM $MgCl_2$, and 10 mM Hepes, pH 7.2, or by ACh or methanethiosulfonate reagents made up in this bath solution. All solutions were at 18°C.

The extent of reaction of MTSEA with a substituted Cys was estimated from the change in the peak currents at a holding potential of −50 mV evoked by test applications of ACh. The initial peak current was measured during a 20-s application of ACh at a concentration approximately 10 times the EC_{50} for the given mutant. After 20 s, the concentration of ACh was increased to 1 mM, and this concentration was applied for 5 min to induce desensitization. At the end of the 5 min, the oocyte was washed with bath solution for 45 s to remove ACh. MTSEA (200 μM to 20 mM) was applied for either 5, 10, or 15 s, depending on the rate of reaction, the oocyte was washed with bath solution for 7 min to reverse desensitization, and the peak current during a 20-s application of the test concentration of ACh was recorded. These steps, starting at the 5-min perfusion with 1 mM ACh immediately after the test response and ending with the next test response, were repeated several times. The peak currents as a function of the cumulative times of exposure to MTSEA were fitted by the first-order reaction rate equation, $I_t = I_\infty + (I_0 - I_\infty)\exp(-k't)$, where I_t is the peak ACh-evoked current after t sec of cumulative MTSEA exposure, I_0 is the initial peak current, I_∞ is the peak current when the reaction is complete, and k' is the pseudo first-order rate constant for the reaction. The second-order rate constant, κ, is given by $\kappa = k'/[\text{MTSEA}]$.

Reaction of Intracellularly Applied MTSEA with Desensitized Receptor. The currents evoked by ACh were recorded from whole-cell, patch-clamped (64) HEK 293 cells expressing ACh receptors, as described (62). MTSEA was applied to the intracellular side of the membrane via the patch pipette, which was filled with 20 mM MTSEA in 140 mM CsCl, 10 mM EGTA, 10 mM Hepes, and 1 mM $MgCl_2$, pH 7.2 (62). Electrode resistance was between 2 and 5 MΩ. The cells were superfused extracellularly with a bath solution of 135 mM NaCl, 5.4 mM KCl, 5 mM Hepes, 1.8 mM $CaCl_2$, and 1 mM $MgCl_2$, pH 7.2. All recordings were made at a holding potential of −50 mV and at 22–26°C.

Within 30 s of establishing continuity between the interior of the pipette and the cytoplasm, we applied ACh extracellularly,

[†]We prefer resting gate to activation gate, for the gate closed in the resting state, consistent with the desensitization gate, the gate closed in the desensitized state.

at a concentration approximately 10 times the EC_{50}, for 10 s, and measured the peak current ($I_{Initial}$). To desensitize the receptors maximally and to maintain the receptors in the desensitized state, we continued for either 10 or 25 min to apply the same concentration of ACh combined with 5 μM proadifen, a desensitizing, noncompetitive inhibitor (65). At the end of this period, we superfused the cell for 5 min with bath solution, which was sufficient to reverse desensitization in HEK 293 cells. Finally, we applied the initial concentration of ACh (with no added proadifen) for 10 s, and we recorded the final peak current, I_{Final}. During the interval starting 1 min after the initial ACh application and ending 1 min before the final ACh application, the voltage clamp was turned off.

The extent of reaction of MTSEA between the two test responses to ACh was estimated as $(1 - I_{Final}/I_{Init})/(1 - I_{Inf}/I_{Init})$. For each receptor mutant, the fraction I_{Inf}/I_{Init} was estimated from the maximal extent of inhibition of the mutant by MTSEA added extracellularly. For each mutant, the extents of reaction of several cells with intracellular MTSEA were determined after 10 min of ACh and proadifen and 5 min of washing, taken as a reaction time of 15 min, and several more cells after 25 min of ACh and proadifen and 5 min of washing, taken as a reaction time of 30 min. In the case of G240C, we also determined the extent of reaction after 5 min of ACh and proadifen and 5 min of washing, taken as a reaction time of 10 min. These results were combined and fit with the above first-order reaction rate equation to estimate the rate constant.

Results

Desensitization and Recovery from Desensitization of Receptors Expressed in Oocytes. The application of ACh at the test concentration to wild-type and mutant receptors in oocytes evoked currents that typically peaked after about 5 s and declined thereafter, reaching one-half of the initial peak current after about 20 s. This is exemplified by the mutant L251C (Fig. 2*A*). The application of 1 mM ACh, starting at 20 s and continuing for 5 min, caused the current amplitude to decline further to a plateau, which was 13% of the peak current in this case and in the range of 4% to 16% overall (Fig. 2*B*). Because a considerable fraction of the receptors was likely to be desensitized already at the time of the initial peak current, the fraction of the total receptors contributing to the plateau current was likely less than 4–16%; i.e., after the 5-min application of ACh, more than 84–96% of the receptors were desensitized.

Despite the extent of desensitization, it was completely reversed by 8 min of washing with bath solution, after which the response to the test concentration of ACh was nearly identical to the initial response before desensitization (Fig. 3*A*). Furthermore, for each of the mutants except L245C and E262C, the cycle of desensitization and recovery could be repeated many times without variation of more than 10% in the response to ACh.

Although after 8 min of washing with bath solution, the receptors were fully recovered from desensitization, after only 45 s of washing, there was relatively little recovery, as measured by I_{Post} (Fig. 2 *A* and *C*). In the mutants, αS248C and αL251C, I_{Post} was about 18% of I_0, whereas I_{Plat} was about 15% of I_0. In several cases, notably wild type, the I_{Post} after a 45-s wash was smaller than I_{Plat}. Thus, after 5 min of 1 mM ACh and 45 s of bath solution, at least 84% of the receptors were desensitized, and the remainder were in the resting state. It was in this mixed state of the receptors that MTSEA was applied.

Reaction of Desensitized Receptors with Extracellularly Applied MTSEA. The protocol to determine the rate of reaction of extracellularly applied MTSEA with desensitized receptors is exemplified by an experiment with the mutant L251C (Fig. 3 *B* and *C*). After a 5-min application of 1 mM ACh and a 45-s wash with bath solution, 200 μM MTSEA was applied for periods from 5 to 15 s (Fig. 3*B*). MTSEA application resulted in a progressive decrease in the test responses. As a function of the cumulative exposure time to MTSEA, the test responses decreased exponentially with a pseudo-first order rate constant of 0.065/s and a half-time of 11 s (Fig. 3*C*). MTSEA itself did not evoke current in any mutant.

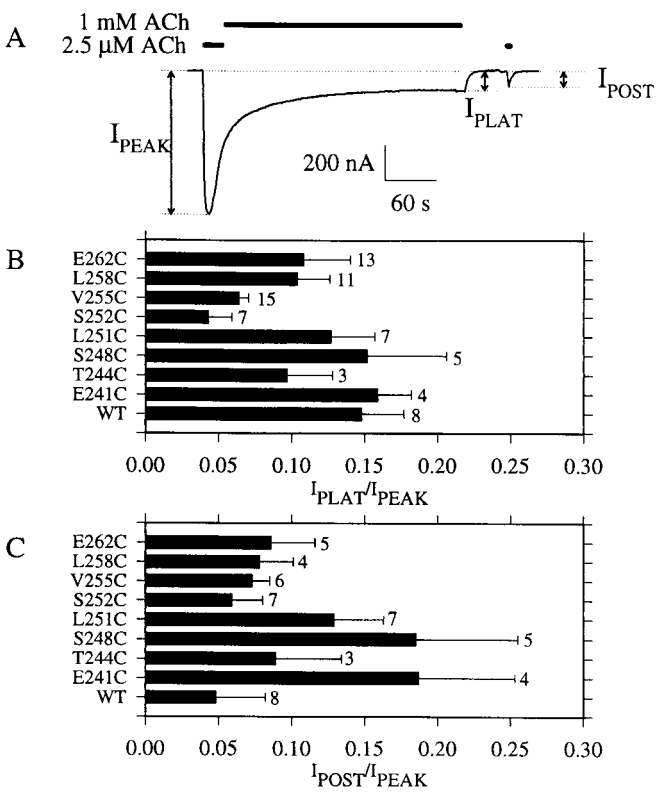

Fig. 2. Desensitization due to prolonged application of 1 mM ACh on receptor. (*A*) A typical recording from an oocyte expressing αL251C and wild-type β, γ, and δ, with I_{PEAK}, I_{PLAT}, and I_{POST} indicated. (*B*) The fraction of current remaining at the end of the desensitizing application of 1 mM ACh, I_{PLAT}/I_{PEAK}, for each mutant and wild type. (*C*) The degree of recovery of current after a 45-s washout of 1 mM ACh, I_{POST}/I_{PEAK}, for each mutant and wild type. Means ± SEM and numbers of experiments are shown.

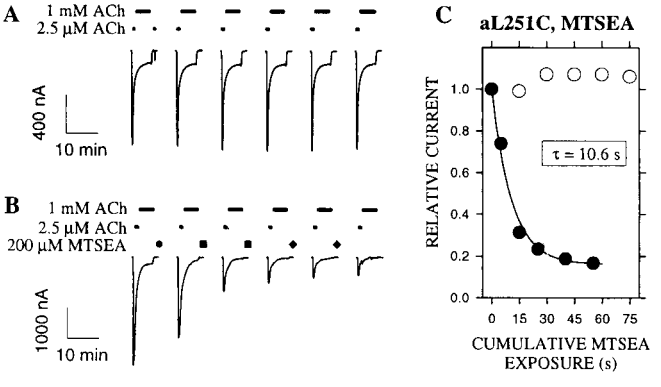

Fig. 3. Measurement of the rate of reaction of MTSEA applied extracellularly to the L251C mutant in the desensitized state. (*A*) Control, no MTSEA. (*B*) Repeated application of MTSEA for 5 s (●), 10 s (■), and 15 s (◆). (*C*) The peak current was normalized and plotted against cumulative time of exposure either to buffer (○, plotted at 15-s intervals) or 200 μM MTSEA (●). The solid line is the least-squares exponential fit to the data (see *Methods*).

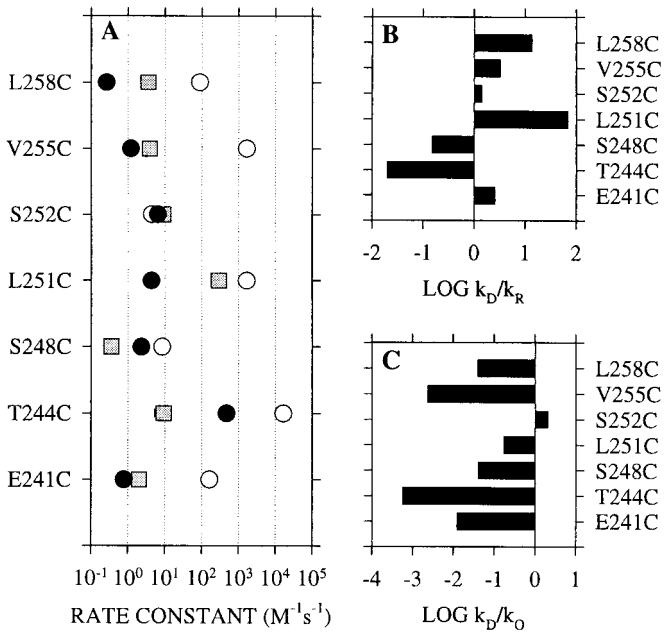

Fig. 4. The second-order rate constants for the reaction of extracellularly applied MTSEA with mutant ACh receptors in different states. (*A*) Second-order rate constants for receptors in the desensitized state (shaded squares; $n = 3$–7; this work) and in the resting (●) and open (○) states (from ref. 61). (*B*) The log of the quotient of the rate constant, k_D, in the desensitized state divided by the rate constant, k_R, in the resting state, for each mutant. (*C*) The log of the quotient of the rate constant, k_D, in the desensitized state divided by the rate constant, k_O, in the open state, for each mutant.

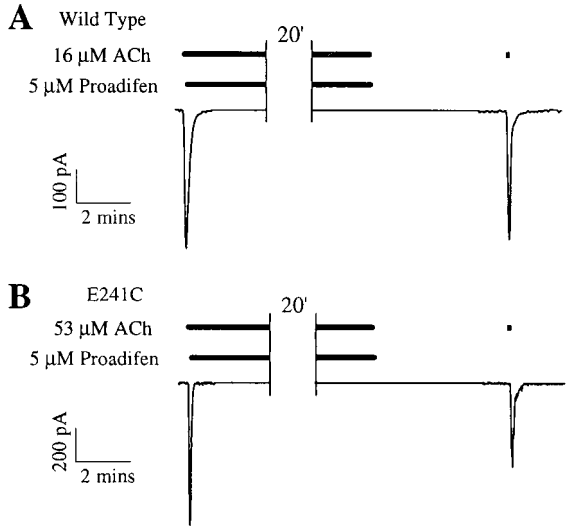

Fig. 5. The effect of the intracellular application of MTSEA to αE241C in the desensitized state. The current evoked by ACh for 10 s was recorded, and the application of ACh continued, with the addition of 5 μM proadifen, for 25 min. The cell was washed for 5 min, and ACh was applied again for 10 s. The voltage clamp was turned off 1 min after the initial application of ACh and turned on again 1 min before the second application of ACh. Traces are shown for wild type (*A*) and αE241C (*B*).

A second-order MTSEA reaction-rate constant was calculated from the pseudo first-order rate constant for each mutant tested (Fig. 4*A*, squares). These can be compared with the rate constants previously determined for the resting (closed) state and the open state (61). For Cys-substituted mutants in the extracellular half of M2, the rate constants were larger in the desensitized state than in the resting state. This was particularly marked for αL251C (Fig. 4*B*). For αS248C and αT244C, the rate constants were smaller in the desensitized state than in the resting state. The reactions of αE241C, flanking the intracellular end of M2, were very slow in both the closed and the desensitized states, with the latter somewhat larger than the former. In all cases, except αS252C, the rate constant in the desensitized state was less than that in the open state (Fig. 4*C*).

For αL245C and αE262C, the rate constants in the resting and the open states were determined previously, but we could not determine the rate constants for the reactions with MTSEA in the desensitized state because there was too much variation in the responses during repeated cycles of desensitization and recovery.

Reactions of Desensitized Receptors with Intracellularly Applied MTSEA. We previously bracketed the location of the gate in the resting (closed) channel by comparing the reactions of MTSEA added extracellularly and intracellularly (62). To locate the gate in the desensitized channel, we also applied MTSEA extracellularly and, separately, intracellularly to the desensitized receptor. Intracellular application was via the patch pipette, which contained 20 mM MTSEA. The reversibility of desensitization (albeit slow) and the continuous presence of MTSEA in the cytoplasm prevented our obtaining from each cell more than an initial response and a final response to estimate the extent of reaction of MTSEA.

Two records, one obtained with wild type (Fig. 5*A*) and the other with αE241C (Fig. 5*B*), illustrate the protocol. Within about 30 s of patch rupture, before MTSEA could reach an effective concentration within the cell (62), a control response to a 10-s application of ACh was measured. This was immediately followed by the extracellular application of 5 μM proadifen, a noncompetitive desensitizing antagonist, in the continued presence of ACh. This resulted in rapid and complete desensitization within 1 min in all cases. After either 10 or 25 min, a 5-min wash removed ACh and proadifen and allowed the receptors to recover from desensitization, after which a final response to a 10-s application of ACh was recorded. In the examples in Fig. 5, the final response was smaller than the initial response in αE241C but not in wild type.

For wild type and three of the mutants probed with intracellular MTSEA, the extent of inhibition after 15 and 30 min, and additionally after 10 min in the case of G240C, are plotted (Fig. 6). In addition, we have plotted the expected time course of inhibition of the ACh-induced current in the open state (dashed line) and the resting state (solid line) based on the rate constants obtained previously for intracellular application of MTSEA to these mutants in HEK 293 cells (62). Although we could not measure the reaction rates precisely, it is clear from the approximate fits (solid lines) that the time courses of the reactions of G240C, E241C, and T244C with intracellular MTSEA in the desensitized state more closely resembles the time courses in the resting state than in the open state. We also applied MTSEA intracellularly to L251C, but in this mutant we detected no reaction.

Protection Against Extracellular MTSEA by QX-314. The quaternary ammonium lidocaine derivatives QX-222 and QX-314 bind within and block conductance through the open channel of the receptor (66–69). QX-222 and QX-314 also protect a number of substituted Cys in the channel-lining M2 segment from reaction with MTSEA in the open state but not in the resting state (70). One substituted Cys that was protected was αL251C. The rate constant for the reaction of extracellular MTSEA with αL251C

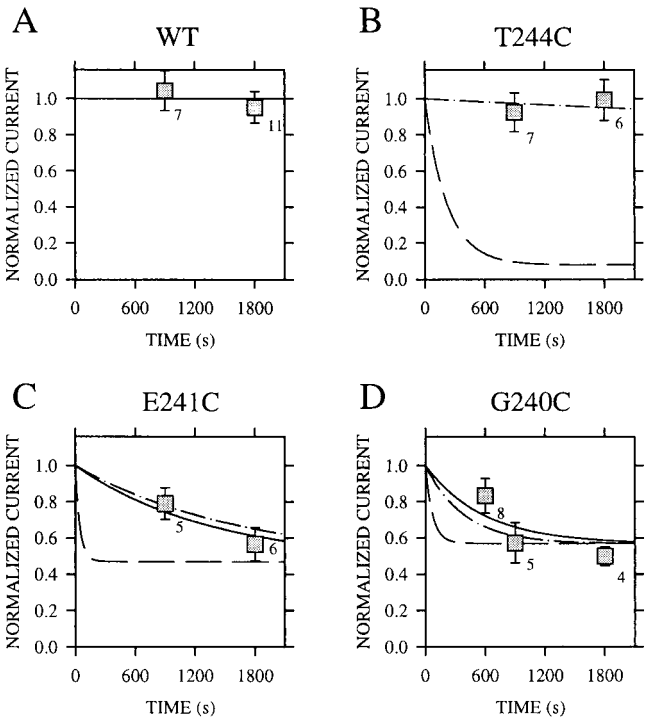

Fig. 6. The time courses of the reactions of intracellular MTSEA. MTSEA was applied as in Fig. 5, for the times indicated along the abscissa. The current evoked by ACh after application of MTSEA was normalized by the initial pre-MTSEA current and plotted against the time elapsed between the two ACh pulses. Effects are shown for wild type (*A*), αT244C (*B*), αE241C (*C*), and αG240C (*D*). The means, standard errors of the mean, and the number of individual time points (and cells) are shown. In *C* and *D*, the data were fit by an exponential decay function with $k = 0.0017/s$ for αG240C and $k = 0.00073/s$ for αE241C (solid lines). Based on the rate constants obtained previously under otherwise similar conditions (62), we plot the time courses of the reactions of intracellular MTSEA with the mutants in the resting state (long dashes) and open state (dash-dots).

in the QX-314-blocked open state was 30% of the rate constant in the unblocked open state. We determined the effect of QX-314 on the reaction of MTSEA with αL251C in the desensitized state. In contrast to the open state, there was no change in the rate of reaction in the presence of 300 μM or 3 mM QX-314 (300 μM QX-314 reduces current in the open state by 50%). In this respect, the desensitized channel resembles the resting channel in not being susceptible to protection by QX-314.

Discussion

What SCAM Tells Us About Channel Structure. The rate constant for the reaction of a given Cys with a methanethiosulfonate (or other reagent) depends on (*i*) the intrinsic reactivity of the reagent, (*ii*) rates of reagent transport to and from the target Cys, and (*iii*) the reactivity of the Cys sulfhydryl (61). Access and egress rates depend on steric and electrostatic factors along the pathways and at the reaction site. The reactivity of the target Cys itself depends on local steric factors and crucially on the extent of deprotonation of the Cys sulfhydryl (63). The electrostatic contributions to the transport rates and the ionization of the sulfhydryl arise from the transmembrane electrostatic potential and from what we called the intrinsic electrostatic potential due to the interaction of the charged reagent with fixed charges and dipoles in the protein surrounding the lumen and in the lumen itself. There is a major energetic cost of transferring a charged or polar reagent from bulk water outside the membrane to the restricted volume and lower effective dielectric constant in the channel lumen. Depending on the charges on the reagent, this positive energy can be compensated by the interaction of the reagent charges with fixed charges in the protein (63).

Despite the energetic cost of transferring a charged reagent from bulk solution to the channel lumen, the cost of transferring it either to the interior of the protein or into the lipid bilayer should be higher. Furthermore, in these latter regions the ionization of the Cys thiol to the reactive thiolate would be suppressed. Thus, the reactions of the charged methanethiosulfonates are expected to be much faster with water-accessible Cys than with buried Cys. When we compare a continuous sequence of Cys mutants in a membrane-spanning segment, the Cys exposed in the channel to water should react much faster than those not exposed, allowing us to identify the residues forming the channel lining and, when the pattern of exposure is regular, to infer the secondary structure of the exposed residues (51, 52). We also can compare the reaction rates of a set of Cys-substituted residues in different functional states; if the rates are different we can conclude that the structures around the residues or along the pathways leading to them are different in the different states.

Although there are several determinants of the rates of reaction in the channel, individual determinants can be examined by taking the ratio of rate constants that vary in that one determinant. We have located the resting gate by comparing the rates of reactions in the resting and open states of Cys substituted for a sequence of residues spanning the gating region with reagent added from one side or the other of the membrane (62). We also have estimated the intrinsic electrostatic contributions to the overall rate constants of the reactions of substituted Cys by comparing the rate constants of differently charged methanethiosulfonates (54, 61, 63).

Reaction Rate Constants in the Different States. We previously found that at many positions in both M1 and M2 of the α subunit and the β subunit, the reactivities of substituted Cys were different in the resting and the open states (51, 52, 58–61). We have now also examined exposed positions in αM2 in the stable desensitized state and find that at many of these positions the rate constants of the reactions of extracellularly applied MTSEA differ in the desensitized state from the rate constants in either the resting state or the open state (Fig. 4*A*). That the rate constants in the desensitized state and the open state are different (Fig. 4*C*) is not surprising, but that the rate constants in the desensitized state and the resting state are quite different from each other is more remarkable because both are nonconducting. The largest differences are in the rates of reaction of L251C, which reacts 70 times more rapidly in the desensitized state than in the resting state, and of T244C, which reacts 50 times more slowly in the desensitized state (Fig. 4*B*). It is notable that in the desensitized state, among the residues tested, L251C reacts with the largest rate constant and S248C, one helical turn below L251C, reacts with the smallest rate constant, 900 times more slowly than L251C (Fig. 4*A*). For L251C and the substituted Cys on its extracellular side the rate constants in the desensitized state are larger than those in the resting state. By contrast, on the intracellular side of L251C, the rate constants for S248C and T244C in the desensitized state are considerably smaller than the rate constants in the resting state (Fig. 4*A*). In the desensitized state, L251 divides M2 into the half toward the extracellular side in which the substituted Cys are more reactive in the desensitized state than in the resting state and the half toward the intracellular side in which the substituted Cys are less reactive in the desensitized state than in the resting state.

The rate constants for the reaction of intracellularly applied MTSEA with Cys substituted for residues in the region of the resting gate are much smaller than the rate constants in the open state and are indistinguishable from the rate constants in the

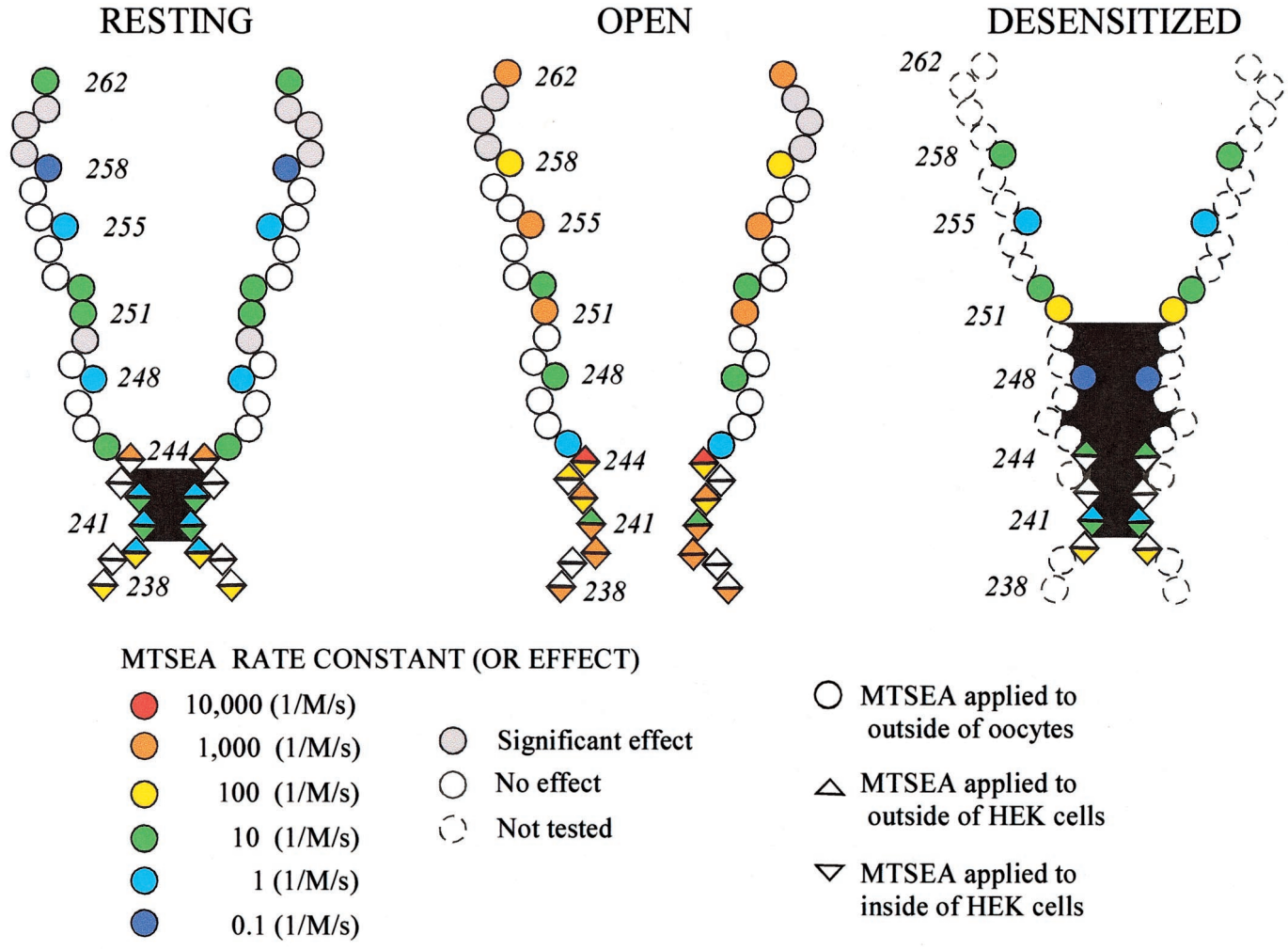

Fig. 7. The reactivities of Cys substituted for the residues in αM2 and the αM1–M2 loop in resting, open, and desensitized states. Two αM2 segments are represented schematically, facing the channel lumen. Where the lumen is black, the channel is relatively impermeable to MTSEA and presumably to inorganic cations. The second-order rate constants are divided into order-of-magnitude bins by rounding log(k) to the nearest integer. The rate constants are color-coded as indicated so that the warmer the color, the greater the rate constant. MTSEA was applied extracellularly by continuous superfusion of the cells, and its concentration was constant and known; hence we could calculate the second-order rate constant by dividing the pseudo first-order rate constants by this concentration. MTSEA was applied intracellularly, however, by diffusion out of the patch pipette, and its concentration at the intracellular surface of the membrane was neither constant nor known, both because of the hydrolysis of MTSEA and the unknown rate of diffusion from the pipette to the membrane. For the purpose of representation, we converted the time constants for the reactions of intracellular MTSEA to second-order rate constants, on the same scale as the second-order rate constants for the reactions with extracellular MTSEA, by multiplying the inverse of the time constants by 28100. For each of G240C, E241C, and K242C, we divided the second-order rate constant for the reaction of extracellular MTSEA by the inverse of the time constant for the reaction of intracellular MTSEA, both reactions in the open state. Log(28100) equals the average of the logs of these quotients. In the case of the desensitized state, all rate constants for the reactions with extracellular MTSEA were obtained in oocytes. Substituted Cys that reacted with MTSEA but for which the rate constants have not been determined are indicated by gray filled circles.

resting state (Fig. 6). In the desensitized state, as in the resting state, intracellular MTSEA does not get into the region of the resting gate or through it to T244C (Fig. 7).

The functional states in which we measured the rate constants were in all cases mixtures of different states (61, 62). When we apply MTSEA in the absence of ACh, both wild-type and mutant receptors are almost entirely in the resting state. The reactions in this state cannot be explained by the very small fraction of the time that the channels open spontaneously. During the short-term application of ACh for seconds, receptors are opening and closing, but also entering the transient desensitized state. Although we cannot rule out the contribution of the transient desensitized state to the reactions early in the application of ACh, the characteristics of the reactions in the immediate presence of ACh and after the long-term application of ACh are so different, that unless the transient desensitized state and the stable desensitized state are very different structurally, the reactions immediately after the addition of ACh can be ascribed mainly to the open state. It is in this admittedly mixed state that we have detected the opening of a gate between αG240 and αT244 and accessibility to this region from both sides of the membrane, and this channel configuration cannot be ascribed to a desensitized state (62). The many differences between the reactions in the stable desensitized state and in the resting state indicate that the former state is not likely to be much contaminated by the latter state.

One particular mutant, αL251C, needs to be considered further, because mutation of the homologous residue, α7L247 to Thr stabilized the open state relative to the resting state and the

desensitized state (37). This result was obtained in a homomeric complex of $\alpha 7$, in which all five subunits bore the mutation. In the heteromeric mouse-muscle receptor, after the aligned Leu in only one or two subunits was mutated, there was some stabilization of the open state relative to the resting state but little effect on desensitization (40, 41). Furthermore, in our experiments, we observed the extent of stable desensitization both before and after the removal of ACh and the addition of MTSEA. The relatively fast rate of reaction of αL251C in the stable desensitized state, much closer to that obtained in the open state than in the resting state (Figs. 4 and 7), cannot be ascribed to contamination either by the open-channel state or by the resting state. We cannot rule out the possibility, however, that the mutation of αL251 (or any other residue) to Cys in itself results in the mutant α subunits adopting a near open-state structure even while the other subunits and the receptor overall were in a nonconducting, desensitized state.

Structural Implications of the Rate Constants. We previously showed that there is a unique gate that blocks the passage of MTSEA in the channel in the resting state but not in the open state; this gate is located between G240 and T244 (62). We argued that this is the resting gate that also blocks the passage of inorganic cations. Notwithstanding the absence of a gate at the extracellular end of the channel, the rate constants of the reactions of extracellularly added MTSEA with the substituted Cys from L245C to L258C are low in the resting state (Fig. 4*A* and ref. 61). The rate constant of the reaction of T244C is, however, quite fast. Low rate constants could result from local steric hindrance around the Cys sulfhydryl, obstructing the formation of a transition-state complex, and a locally low dielectric constant, suppressing the ionization of the sulfhydryl and decreasing the residence time in the vicinity of the Cys of charged MTSEA. Residues in the N-terminal third of the M1 membrane-spanning segment, toward its extracellular end, are also exposed in the channel and could contribute to the local obstruction of the substituted Cys in the half of M2 toward its extracellular end (58, 59). The sulfhydryl of substituted Cys could be sterically hindered, and at the same time the channel lumen itself could be wide enough to allow rapid passage of MTSEA.

Another influence that would lower the rate of reaction of MTSEA with Cys in the more extracellular half of M2 in the resting state is the positive intrinsic electrostatic potential in the lumen, for example around αL258, +50 mV in the resting state compared with −25 mV in the open state (61). This would decrease the probability of MTSEA residing around αL258C about 20-fold; however, this residue reacted 400 times more slowly with MTSEA in the resting state than in the open state, so that the electrostatic potential is not the only influence.

A low effective dielectric constant and an unfavorable intrinsic electrostatic potential also might account for the lack of protection afforded by the quaternary ammonium lidocaine derivative QX-314 against the reaction of L251C with MTSEA in both the resting (70) and desensitized states (see *Results*). Also, a local obstruction toward the extracellular end of the channel could possibly block access by QX-314 but not of the smaller MTSEA. QX-314 does protect L251C against MTSEA in the open state (70).

In the desensitized state, the rate constants for the reactions of extracellularly applied MTSEA with L258C, V255C, and S252C are all low, but the rate constant of the reaction of L251C is moderately high, 75 times that of V255C above. Clearly there is no desensitization gate above L251C. On the other hand, S248C and T244C below L251C react even more slowly in the desensitized state than in the resting state. These low rates could reflect greater local obstruction of these positions in the desensitized state than in the resting state. The very low rates of reaction of G240C, E241C, and T244C with MTSEA added intracellularly, as well as extracellularly, imply that the gate between G240C and T244C is closed in the desensitized state just as it is in the resting state. Possibly this resting gate is extended in the desensitized state to occlude T244 and S248 (Fig. 7). L251, also, could contribute to the desensitization gate, because if the Leu side chains are extended into the lumen, then a Cys substituted for one of them might be quite reactive. We have inferred that αL251 and the other aligned Leu are more exposed in the water-filled channel lumen in the open state than in the resting state (51, 60), but the five aligned Leu do not obstruct the channel in the open state. In the desensitized state, αL251C reacts 70 times faster than in the resting state and only six times slower than in the open state. In the desensitized state also, the side chains of αL251 and the aligned Leu are exposed in the lumen but could be close enough together to obstruct the channel and contribute to the desensitization gate.

This possibility is consistent with the previous suggestion that in the neuronal ACh receptor composed of five $\alpha 7$ subunits the five Leu (L247) homologous to L251 in muscle-type α subunit form the desensitization gate (37). Our results indicate, however, that in muscle-type receptor, αL251 and the aligned Leu in the other subunits do not form the desensitization gate alone. If L251 and the aligned Leu in the other subunits contribute to the desensitization gate, they are likely to be part of the extension of the resting state gate (Fig. 7). Our present and previous results (62) are not consistent with the suggestion that αL251 and the aligned Leu in the other subunits form the gate in the resting state (21).

Auerbach and Akk (7) suggested that there are two separate gates in the channel, a resting gate and a desensitization gate. They suggested further that in the resting state, the resting (activation) gate is closed and the desensitization gate is open and that in the agonist-occupied desensitized state the resting gate is open and the desensitization gate is closed. Our results support the idea that the gate structures are not identical in the resting state and the desensitized state but not the ideas that they are entirely separate or that the resting gate remains open when the desensitization gate closes. Auerbach and Akk analyzed the transient desensitized state that occurs on the time scale of 0.1–1 s, whereas we analyzed the stable desensitized state after minutes in ACh. Conceivably, in the transition from the open state to the first stage of desensitization, the region from T244 to L251 could close before the region between G240 and T244.

A highly hydrophobic photolabel, 3-trifluoromethyl-3-(*m*-iodophenyl)diazirine, reacted in the resting state with residues in β and δ aligned with αL251 and αV255 and with residues aligned with αT244 and αS248 in the desensitized state (26, 27). These results were taken as evidence for a resting gate aligned with αL251; they are also consistent, however, with the side chains of αL251 and αV255 being in a more hydrophobic environment than αT244 in the resting state and that αT244 and αS248 are in a more hydrophobic environment than αL251 in the desensitized state (Fig. 7). This label could intercalate into clusters of hydrophobic side chains.

In summary, our application of SCAM to the ACh receptor in the resting, open, and desensitized states has identified structural differences in the channel lining in these states and the residues likely to form the closed gates in the resting state and the desensitized state.

We thank Drs. Anthony Auerbach, Claudio Grosman, H. Ronald Kaback, and Juan Pascual for valuable discussions. This work was supported by Research Grant NS07065 from the National Institute of Neurological Disorders and Stroke.

1. Katz, B. & Thesleff, S. (1957) *J. Physiol. (London)* **138,** 63–80.
2. Reynolds, J. A. & Karlin, A. (1978) *Biochemistry* **17,** 2035–2038.
3. Karlin, A. & Akabas, M. H. (1995) *Neuron* **15,** 1231–1244.
4. Cachelin, A. B. & Colquhoun, D. (1989) *J. Physiol. (London)* **415,** 159–188.
5. Dilger, J. P. & Liu, Y. (1992) *Pflügers Arch.* **420,** 479–485.
6. Franke, C., Parnas, H., Hovav, G. & Dudel, J. (1993) *Biophys. J.* **64,** 339–356.
7. Auerbach, A. & Akk, G. (1998) *J. Gen. Physiol.* **112,** 181–197.
8. Jones, M. V. & Westbrook, G. L. (1996) *Trends Neurosci.* **19,** 96–101.
9. Ochoa, E. L., Chattopadhyay, A. & McNamee, M. G. (1989) *Cell. Mol. Neurobiol.* **9,** 141–178.
10. Sakmann, B., Patlak, J. & Neher, E. (1980) *Nature (London)* **286,** 71–73.
11. Heidmann, T., Bernhardt, J., Neumann, E. & Changeux, J. P. (1983) *Biochemistry* **22,** 5452–5459.
12. Neubig, R. R., Boyd, N. D. & Cohen, J. B. (1982) *Biochemistry* **21,** 3460–3467.
13. Hess, G. (1993) *Biochemistry* **32,** 989–1000.
14. Magleby, K. L. & Pallotta, B. S. (1981) *J. Physiol. (London)* **316,** 225–250.
15. Feltz, A. & Trautman, A. (1982) *J. Physiol. (London)* **322,** 257–272.
16. Chesnut, T. J. (1993) *J. Physiol. (London)* **336,** 229–241.
17. Lester, R. A. & Dani, J. A. (1995) *J. Neurophysiol.* **74,** 195–206.
18. Heidmann, T. & Changeux, J. P. (1980) *Biochem. Biophys. Res. Commun.* **97,** 889–896.
19. Neubig, R. R. & Cohen, J. B. (1980) *Biochemistry* **19,** 2770–2779.
20. Unwin, N., Toyoshima, C. & Kubalek, E. (1988) *J. Cell. Biol.* **107,** 1123–1138.
21. Unwin, N. (1995) *Nature (London)* **373,** 37–43.
22. Unwin, N. (1996) *J. Mol. Biol.* **257,** 586–596.
23. Kao, P. N. & Karlin, A. (1986) *J. Biol. Chem.* **261,** 8085–8088.
24. Damle, V. N. & Karlin, A. (1980) *Biochemistry* **19,** 3924–3932.
25. Galzi, J. L., Revah, F., Bouet, F., Menez, A., Goeldner, M., Hirth, C. & Changeux, J. P. (1991) *Proc. Natl. Acad. Sci. USA* **88,** 5051–5055.
26. McCarthy, M. P. & Moore, M. A. (1992) *J. Biol. Chem.* **267,** 7655–7663.
27. White, B. H. & Cohen, J. B. (1992) *J. Biol. Chem.* **267,** 15770–15783.
28. Blanton, M. P., McCardy, E. A., Huggins, A. & Parikh, D. (1998) *Biochemistry* **37,** 14545–14555.
29. Middleton, R. E., Strnad, N. P. & Cohen, J. B. (1999) *Mol. Pharmacol.* **56,** 290–299.
30. Pedersen, S. E., Sharp, S. D., Liu, W. S. & Cohen, J. B. (1992) *J. Biol. Chem.* **267,** 10489–10499.
31. Cox, R. N., Kaldany, R. R., DiPaola, M. & Karlin, A. (1985) *J. Biol. Chem.* **260,** 7186–7193.
32. Heidmann, T. & Changeux, J. P. (1986) *Biochemistry* **25,** 6109–6113.
33. DiPaola, M., Kao, P. N. & Karlin, A. (1990) *J. Biol. Chem.* **265,** 11017–11029.
34. Sine, S. M., Ohno, K., Bouzat, C., Auerbach, A., Milone, M., Pruitt, J. N. & Engel, A. G. (1995) *Neuron* **15,** 229–239.
35. Corringer, P. J., Bertrand, S., Bohler, S., Edelstein, S. J., Changeux, J. P. & Bertrand, D. (1998) *J. Neurosci.* **18,** 648–657.
36. Osaka, H., Sugiyama, N. & Taylor, P. (1998) *J. Biol. Chem.* **273,** 12758–12765.
37. Revah, F., Bertrand, D., Galzi, J. L., Devillers-Thiery, A., Mulle, C., Hussy, N., Bertrand, S., Ballivet, M. & Changeux, J. P. (1991) *Nature (London)* **353,** 846–849.
38. Bertrand, D., Devillers-Thiery, A., Revah, F., Galzi, J. L., Hussy, N., Mulle, C., Bertrand, S., Ballivet, M. & Changeux, J. P. (1992) *Proc. Natl. Acad. Sci. USA* **89,** 1261–1265.
39. Devillers-Thiery, A., Galzi, J. L., Bertrand, S., Changeux, J. P. & Bertrand, D. (1992) *NeuroReport* **3,** 1001–1004.
40. Filatov, G. N. & White, M. M. (1995) *Mol. Pharmacol.* **48,** 379–384.
41. Labarca, C., Nowak, M. W., Zhang, H., Tang, L., Deshpande, P. & Lester, H. A. (1995) *Nature (London)* **376,** 514–516.
42. Weiland, S., Witzemann, V., Villarroel, A., Propping, P. & Steinlein, O. (1996) *FEBS Lett.* **398,** 91–96.
43. Kuryatov, A., Gerzanich, V., Nelson, M., Olale, F. & Lindstrom, J. (1997) *J. Neurosci.* **17,** 9035–9047.
44. Milone, M., Wang, H. L., Ohno, K., Fukudome, T., Pruitt, J. N., Bren, N., Sine, S. M. & Engel, A. G. (1997) *J. Neurosci.* **17,** 5651–5665.
45. Bertrand, S., Weiland, S., Berkovic, S. F., Steinlein, O. K. & Bertrand, D. (1998) *Br. J. Pharmacol.* **125,** 751–760.
46. Buckingham, S. D., Adcock, C., Sansom, M. S., Sattelle, D. B. & Baylis, H. A. (1998) *Br. J. Pharmacol.* **124,** 747–755.
47. Campos-Caro, A., Rovira, J. C., Vicente-Agullo, F., Ballesta, J. J., Sala, S., Criado, M. & Sala, F. (1997) *Biochemistry* **36,** 2709–2715.
48. Wang, H. L., Milone, M., Ohno, K., Shen, X. M., Tsujino, A., Batocchi, A. P., Tonali, P., Brengman, J., Engel, A. G. & Sine, S. M. (1999) *Nat. Neurosci.* **2,** 226–233.
49. Lee, Y. H., Li, L., Lasalde, J., Rojas, L., McNamee, M., Ortiz-Miranda, S. I. & Pappone, P. (1994) *Biophys. J.* **66,** 646–653.
50. Swope, S. L., Qu, Z. & Huganir, R. L. (1995) *Ann. N.Y. Acad. Sci.* **757,** 197–214.
51. Akabas, M. H., Stauffer, D. A., Xu, M. & Karlin, A. (1992) *Science* **258,** 307–310.
52. Akabas, M. H., Kaufmann, C., Archdeacon, P. & Karlin, A. (1994) *Neuron* **13,** 919–927.
53. Karlin, A. & Akabas, M. H. (1998) *Methods Enzymol.* **293,** 123–145.
54. Stauffer, D. A. & Karlin, A. (1994) *Biochemistry* **33,** 6840–6849.
55. Javitch, J. A., Li, X., Kaback, J. & Karlin, A. (1994) *Proc. Natl. Acad. Sci. USA* **91,** 10355–10359.
56. Javitch, J. A., Fu, D., Chen, J. & Karlin, A. (1995) *Neuron* **14,** 825–831.
57. Roberts, D. D., Lewis, S. D., Ballou, D. P., Olson, S. T. & Shafer, J. A. (1986) *Biochemistry* **25,** 5595–5601.
58. Akabas, M. H. & Karlin, A. (1995) *Biochemistry* **34,** 12496–12500.
59. Zhang, H. & Karlin, A. (1997) *Biochemistry* **36,** 15856–15864.
60. Zhang, H. & Karlin, A. (1998) *Biochemistry* **37,** 7952–7964.
61. Pascual, J. M. & Karlin, A. (1998) *J. Gen. Physiol.* **111,** 717–739.
62. Wilson, G. G. & Karlin, A. (1998) *Neuron* **20,** 1269–1281.
63. Wilson, G. G., Pascual, J. M., Brooijmans, N., Murray, D. & Karlin, A. (2000) *J. Gen. Physiol.* **115,** 93–106.
64. Hamill, O. P., Marty, A., Neher, E., Sakmann, B. & Sigworth, F. J. (1981) *Pflügers Arch.* **391,** 85–100.
65. Boyd, N. D. & Cohen, J. B. (1984) *Biochemistry* **23,** 4023–4033.
66. Neher, E. & Steinbach, J. H. (1978) *J. Physiol. (London)* **277,** 153–176.
67. Neher, E. (1983) *J. Physiol. (London)* **339,** 663–678.
68. Horn, R., Brodwick, M. S. & Dickey, W. D. (1980) *Science* **210,** 205–207.
69. Charnet, P., Labarca, C., Leonard, R. J., Vogelaar, N. J., Czyzyk, L., Gouin, A., Davidson, N. & Lester, H. A. (1990) *Neuron* **4,** 87–95.
70. Pascual, J. M. & Karlin, A. (1998) *J. Gen. Physiol.* **112,** 611–621.